© 2016. Published by The Company of Biologists Ltd | Journal of Cell Science (2016) 129, 1815-1830 doi:10.1242/jcs.185009

RESEARCH ARTICLE

Cdk5–Foxo3 axis: initially neuroprotective, eventually neurodegenerative in Alzheimer's disease models

Chun Shi[1,*], Keith Viccaro[1], Hyoung-gon Lee[2] and Kavita Shah[1,‡]

ABSTRACT

Deregulated Cdk5 causes neurotoxic amyloid beta peptide (Aβ) processing and cell death, two hallmarks of Alzheimer's disease, through the Foxo3 transcriptional factor in hippocampal cells, primary neurons and an Alzheimer's disease mouse model. Using an innovative chemical genetic screen, we identified Foxo3 as a direct substrate of Cdk5 in brain lysates. Cdk5 directly phosphorylates Foxo3, which increased its levels and nuclear translocation. Nuclear Foxo3 initially rescued cells from ensuing oxidative stress by upregulating MnSOD (also known as SOD2). However, following prolonged exposure, Foxo3 upregulated Bim (also known as BCL2L11) and FasL (also known as FASLG) causing cell death. Active Foxo3 also increased Aβ(1–42) levels in a phosphorylation-dependent manner. These events were completely inhibited either by expressing phosphorylation-resistant Foxo3 or by depleting Cdk5 or Foxo3, highlighting a key role for Cdk5 in regulating Foxo3. These results were confirmed in an Alzheimer's disease mouse model, which exhibited increased levels and nuclear localization of Foxo3 in hippocampal neurons, which preceded neurodegeneration and Aβ plaque formation, indicating this phenomenon is an early event in Alzheimer's disease pathogenesis. Collectively, these results show that Cdk5-mediated phospho-regulation of Foxo3 can activate several genes that promote neuronal death and aberrant Aβ processing, thereby contributing to the progression of neurodegenerative pathologies.

KEY WORDS: Cdk5, Foxo3, Alzheimer's disease, Neurodegeneration, Neuroprotection

INTRODUCTION

Alzheimer's disease is a debilitating neurological disorder that currently affects an estimated 5.3 million Americans. Recent failure of several high-profile drugs aimed at slowing the progression of the disease in Phase 3 clinical trials highlight the need to fully understand the biochemical mechanisms that drive Alzheimer's disease pathogenesis. The only available drugs are acetylcholinesterase inhibitors and *N*-methyl *D*-aspartate receptor antagonists, which, at best, delay disease progression, but do not prevent neurodegeneration (Sun et al., 2012). In this study, we focused on cyclin-dependent kinase-5 (Cdk5), which is deregulated in Alzheimer's disease and contributes significantly to its three hallmarks: amyloid beta peptide (Aβ) plaques, neurofibrillary tangles (NFT) and extensive neurodegeneration.

Cdk5 has a high similarity to other Cdks; however, it possesses unique activation pathways and distinct cellular functions (Dhavan and Tsai, 2001; Shah and Lahiri, 2014). Unlike other Cdks, Cdk5 does not participate in cell cycle regulation in proliferating cells, although it can aberrantly activate different components of the cell cycle in post-mitotic neurons, resulting in death under pathological conditions (Chang et al., 2012). Furthermore, Cdk5 is not activated by the canonical cyclins, but binds to its own specific partners, p35 (also known as CDK5R1) and p39 (also known as CDK5R2). Expression of p35 is almost ubiquitous, whereas p39 is specifically expressed in the central nervous system.

Cdk5 plays a pivotal role in neuronal development by regulating neuronal migration, neurite outgrowth, axon guidance and synapse formation (McLinden et al., 2012). In adults, Cdk5 is crucial for neurotransmission, synaptic plasticity and homeostasis, drug addiction and long-term behavioral changes (Bibb et al., 2001; Hawasli et al., 2007; Hisanaga and Endo, 2010).

In many neurodegenerative diseases, such as Alzheimer's disease, Parkinson's disease, amyotrophic lateral sclerosis and ischemic stroke, Cdk5 is aberrantly hyper-activated and becomes destructive and neurotoxic (Fischer et al., 2005; Shukla et al., 2012; Meyer et al., 2014). A variety of neurotoxic insults such as exposure to Aβ, excitotoxicity, ischemia and oxidative stress disrupt the intracellular Ca^{2+} homeostasis in neurons, thereby leading to the activation of calpain, which cleaves p35 into p25 and p10. The Cdk5–p25 complex exhibits higher kinase activity *in vitro* than the Cdk5–p35 complex. Furthermore, p25 has a 6-fold longer half-life compared to p35 and lacks the membrane-anchoring signal, which results in its constitutive activation and, most importantly, mis-localization of the Cdk5–p25 complex to the cytoplasm and the nucleus. There, Cdk5–p25 is able to access and phosphorylate a variety of atypical pathological targets, which ultimately trigger a cascade of neurotoxic pathways that culminate in neuronal death (Sun et al., 2009; Chang et al., 2010). Hyperactive Cdk5–p25 hyperphosphorylates tau (also known as MAPT), which aggregates to form the neurofibrillary tangles observed in Alzheimer's disease. Furthermore, hyperphosphorylation of tau and CRMP2 (also known as DPYSL2) by Cdk5 also significantly impairs axonal transport, causing neuronal death (Hensley et al., 2011). Similarly, deregulation of Cdk5 by ectopic expression of p25 results in increased pausing of mitochondria in neurons (Morel et al., 2010). The resulting mitochondrial 'traffic jam' causes a drop in ATP levels, resulting in synaptic dysfunction and ultimately neuronal death (Whiteman et al., 2009).

In this study, we uncovered a new mechanism by which deregulated Cdk5 causes neurotoxic Aβ processing and cell death, two hallmarks of Alzheimer's disease, by directly phosphorylating the FOXO3a (human isoform) transcriptional factor. Using an innovative chemical genetic screen, we identified transcription

[1]Department of Chemistry and Purdue University Center for Cancer Research, Purdue University, 560 Oval Drive, West Lafayette, IN 47907, USA. [2]Department of Pathology, Case Western Reserve University School of Medicine, Iris S. Bert L. Wolstein Research Building, 2103 Cornell Road, Room 5123, Cleveland, OH 44106, USA.
*Present address: Department of Anatomy, Guangzhou Medical University, Guangzhou, Guangdong, China.

‡Author for correspondence (shah23@purdue.edu)

Received 16 December 2015; Accepted 3 March 2016

Journal of Cell Science

Journal of Cell Science (2016) 129, 1815-1830 doi:10.1242/jcs.185009

factor Foxo3 (murine isoform) as a new substrate of Cdk5 kinase in mouse brain lysates. Among the four mammalian forkhead transcription factors of the O class (FOXOs), FOXO1 and FOXO3a are highly expressed in the human brain, specifically in areas vulnerable to Alzheimer's disease (Hoekman et al., 2006). FOXOs regulate diverse cellular processes including oxidative stress resistance and apoptosis (Fukunaga et al., 2005; Klotz et al., 2015). FOXOs are activated by oxidative stress; however, their roles in the pathogenesis of Alzheimer's disease remain unclear. In this study, we investigated the mechanism of Foxo3 activation and its consequences in a mouse hippocampal cell line (HT22 cells), mouse primary neurons and a p25 transgenic mouse model of Alzheimer's disease.

RESULTS

FOXO3a is a direct substrate of Cdk5

The chemical genetic approach utilizes an engineered kinase, which in the presence of a radioactive orthogonal ATP analog [e.g. N^6-(phenethyl) ATP], specifically transfers the radioactive tag (^{32}P) to its substrates. The modified pocket in the engineered kinase is created by replacing a conserved bulky residue in the active site with a glycine or alanine residue. The complementary substituent on ATP is created by attaching bulky groups at the N-6 position of ATP. These ATP analogs are not accepted by wild-type kinases due to steric effects, permitting unbiased identification of direct substrates of the engineered kinase in a global environment (Shah and Vincent, 2005; Kim and Shah, 2007; Johnson et al., 2011; Johnson et al., 2012). Importantly, the sensitized allele created by this mutation has identical substrate specificity to the wild-type kinase. Using the aforementioned design criteria, we generated an analog-sensitive mutant of Cdk5 (named Cdk5-as1) that efficiently accepted N-6-Phenethyl-ATP (PE-ATP) as the orthogonal ATP analog. Using Cdk5-as1 and [^{32}P]PE-ATP, we have identified several novel Cdk5 substrates, including GM130 (also known as GOLGA2), peroxiredoxin 1, peroxiredoxin 2, lamin A, lamin B, Cdc25A, Cdc25B and Cdc25C (Sun et al., 2008a,b; Chang et al., 2011, 2012). In this study, we focused on Cdk5-mediated regulation of Foxo3 signaling. As proteomics screen can often lead to false positives, we tested whether Cdk5 directly phosphorylates FOXO3a using an *in vitro* kinase assay. Cdk5 directly phosphorylates FOXO3a, confirming the result obtained from the chemical genetic screen (Fig. 1A).

Cdk5 and Foxo3 associate in HT22 cells

To uncover the significance of Foxo3 phosphorylation by Cdk5, we determined whether these two proteins associate with each other in HT22 cells under normal and/or neurotoxic conditions. We chose glutamate as the neurotoxic signal. Glutamate excitotoxicity is a major contributor to Alzheimer's disease pathogenesis. We isolated a Cdk5 immune complex and analyzed Foxo3 levels in untreated HT22 cells, which revealed no association of Cdk5 with Foxo3 (Fig. 1B, lane 1). However, when these cells were treated with glutamate, a time-dependent increase in the association between Cdk5 and Foxo3 was observed in Cdk5 immune complexes. These results suggest that Cdk5 and Foxo3 associate only under neurotoxic conditions (Fig. 1B).

Cdk5 regulates the subcellular localization of Foxo3 in HT22 cells

Association of Cdk5 and Foxo3 upon glutamate treatment prompted us to investigate their subcellular localization in HT22 cells. In untreated cells, Cdk5 was predominantly cytosolic, consistent with our previous findings (Sun et al., 2009). Surprisingly, Foxo3 was also present in the cytoplasm although it evidently did not associate with Cdk5 (Fig. 2A). Exposure to glutamate resulted in increased nuclear translocation of both Cdk5 and Foxo3 in a time-dependent manner (Fig. 2A,B). After 6–12 h of glutamate treatment, more than 80% cells displayed nuclear Cdk5 and Foxo3. Notably, when Cdk5 was inhibited using the small-molecule inhibitor roscovitine, both Foxo3 and Cdk5 remained in the cytoplasm, suggesting that Cdk5 and Foxo3 not only colocalize, but that Cdk5 also regulates the subcellular localization of Foxo3 in HT22 cells presumably through its kinase activity (Fig. 2A,B).

To further validate these results, we conducted cytosolic and nuclear fractionation of control and HT22 cells exposed to glutamate for various times. Similar to the results obtained using immunofluorescence, cellular fractionation also revealed a time-dependent increase in the translocation of Cdk5 and Foxo3 to the nucleus, which increased with glutamate exposure time (Fig. 2C). Cdk5 inhibition using roscovitine prevented this translocation, which further validates that Cdk5 kinase activity is responsible for the migration of Foxo3 to the nucleus (Fig. 2D).

Cdk5 knockdown inhibits nuclear translocation of Foxo3

Although roscovitine is a highly potent and the most commonly used inhibitor of Cdk5, it is not monospecific and inhibits Cdk1 and Cdk2 with equal potency. Therefore, we also knocked down Cdk5 using Cdk5-specific short hairpin RNA (shRNA) and investigated the subcellular localization of Foxo3 in glutamate-treated HT22 cells (Fig. 2E). Depletion of Cdk5 completely inhibited the translocation of Foxo3 to the nucleus upon glutamate treatment (analyzed up to 12 h) further supporting the results obtained using roscovitine (Fig. 2F,G). Finally, we also generated nuclear and cytosolic fractions of control, glutamate-treated and Cdk5-shRNA-treated cells, which too revealed complete inhibition of Foxo3 translocation in the absence of Cdk5 (Fig. 2H). Collectively, these results demonstrate that deregulated Cdk5 controls the migration of Foxo3 to the nucleus upon deregulation. Importantly, cellular fractionation experiments revealed increased levels of lamin A in the cytosolic fraction of glutamate-treated cells (Fig. 2C), but significantly less levels in Cdk5-inhibited (Fig. 2D) or Cdk5-depleted cells (Fig. 2H). This finding is consistent with our previous

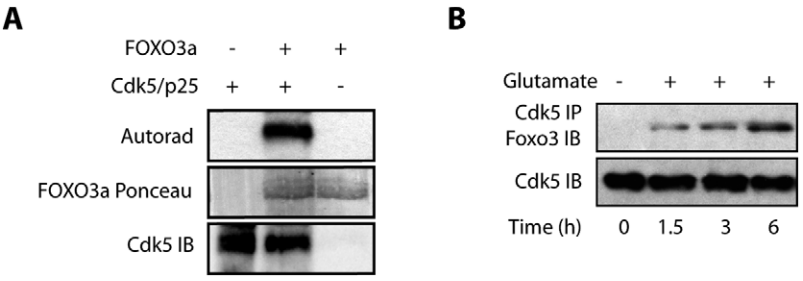

Fig. 1. (A) FOXO3a is a direct substrate of Cdk5. The Cdk5–p25 complex (Cdk5/p25) was subjected to kinase assay with either [^{32}P]ATP alone (lane 1), or with 6×-His–FOXO3a and [^{32}P]ATP (lane 2) for 15 min. Lane 3 shows FOXO3a incubated with [^{32}P]ATP. (B) Glutamate stimulates association of Cdk5 and Foxo3. Cdk5 was immunoprecipitated (IP) from either control or glutamate-treated HT22 cells (for 0–6 h), and the association of Cdk5 and Foxo3 was analyzed. IB, immunoblotting. Each experiment was repeated at least three independent times.

Journal of Cell Science (2016) 129, 1815-1830 doi:10.1242/jcs.185009

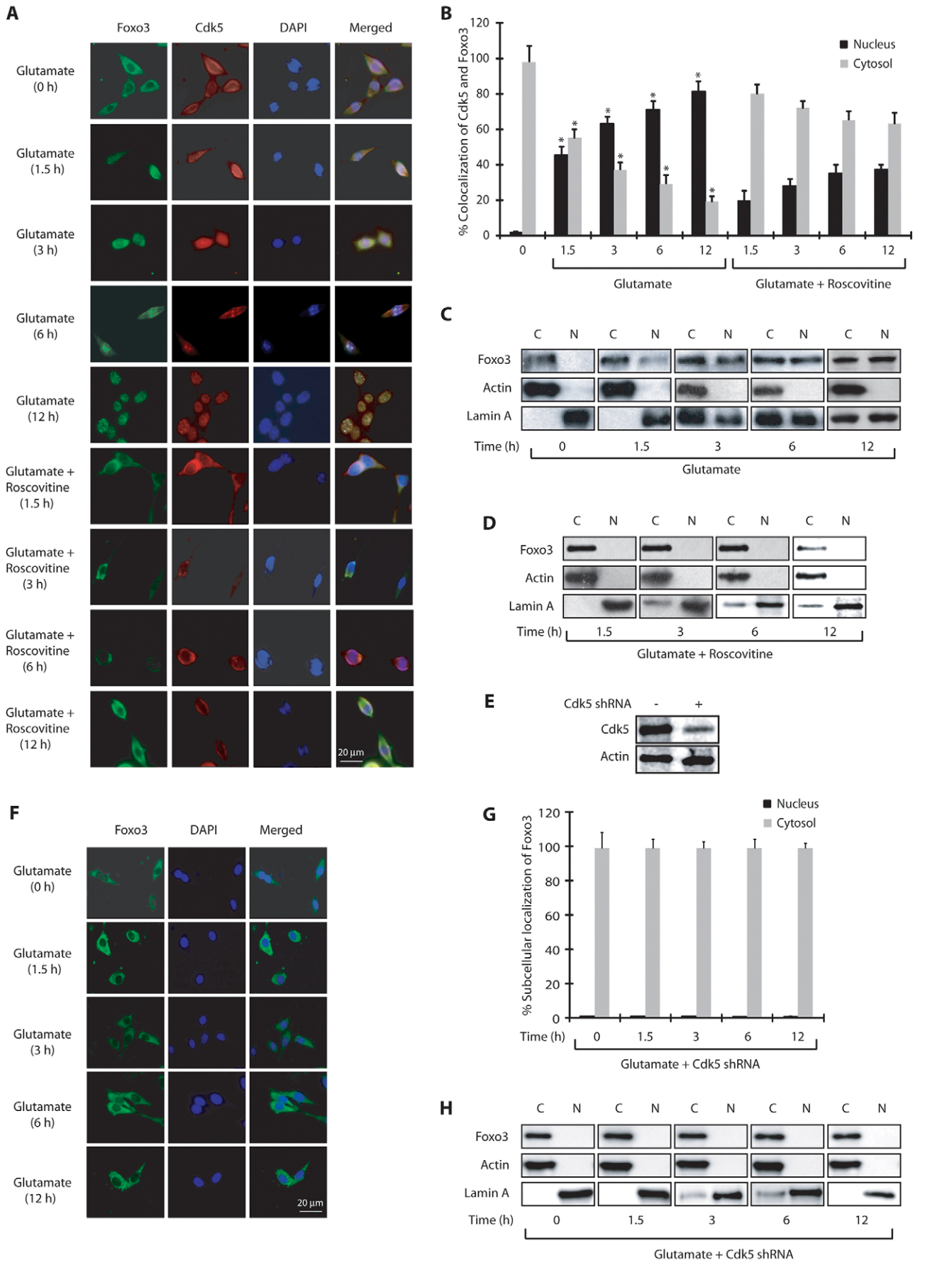

Fig. 2. See next page for legend.

Journal of Cell Science (2016) 129, 1815-1830 doi:10.1242/jcs.185009

Fig. 2. Cdk5 promotes nuclear localization of Foxo3 upon glutamate stimulation. (A) Glutamate stimulates nuclear translocation of Cdk5 and Foxo3. HT22 cells were treated with glutamate for 0–12 h with or without roscovitine, followed by immunostaining as described in the Materials and Methods. Representative pictures are shown. (B) Percentage of cells showing nuclear translocation of Cdk5 and Foxo3a. At least 100 cells from 10 random frames were counted. *P<0.01, compared with untreated HT22 cells (Student's t-test). (C,D) Subcellular fractionation of Foxo3 in glutamate-treated HT22 cells in the absence or presence of roscovitine as described in the Materials and Methods. Actin is the cytoplasmic marker and lamin A is the nuclear marker. N, nuclear fraction; C, cytoplasmic fraction. (E) Scrambled- and Cdk5-shRNA-infected HT22 cells (F) Cdk5 knockdown inhibits nuclear translocation of Foxo3. HT22 cells were treated with Cdk5 shRNA for 30 h, followed by glutamate treatment for 0–12 h. (G) The percentage of cells showing nuclear translocation of Foxo3. (H) Cdk5 shRNA infected HT22 cells were treated with glutamate (0–12 h) and –fractionated as described in the Materials and Methods. Actin is the cytoplasmic marker and lamin A is the nuclear marker. N, nuclear fraction; C, cytoplasmic fraction. Graphical results are mean±s.e.m. Each experiment was repeated at least three independent times.

report that showed rapid dispersion of nuclear lamina in glutamate-treated cells triggered by Cdk5-mediated phosphorylation of lamin A and lamin B1 (Chang et al., 2011).

Cdk5 phosphorylates FOXO3a at S43, S173, S294 and S325

To gain insight into glutamate-triggered regulation of Foxo3, we examined Cdk5-mediated phosphorylation sites on FOXO3a (human isoform). Cdk5 is a proline-directed kinase which preferentially phosphorylates SP and TP sites with adjacent basic residues. Based on this preference, we generated multiple phosphorylation-resistant mutants of FOXO3a and subjected them to kinase assays using Cdk5–p25. FOXO3a was phosphorylated at S43, S173, S294 and S325 (human numbering) by Cdk5–p25 (Fig. 3A). To confirm that these were the only sites that were phosphorylated by Cdk5, we generated the corresponding (S43A, S173A, S294A, S325A) quadruple mutant (abbreviated as 4A-FOXO3a) and subjected it to a kinase assay using Cdk5–p25. Unlike wild-type FOXO3a, 4A-FOXO3a was not phosphorylated by Cdk5–p25 suggesting that these are the only Cdk5 sites on FOXO3a (Fig. 3B).

Cdk5-mediated FOXO3 phosphorylation triggers its nuclear translocation

To uncover the consequences of Cdk5-mediated phosphorylation of FOXO3a, we generated a wild-type (wt)-FOXO3a-expressing stable HT22 cell line. Similar to HT22 cells, FOXO3a-HT22 cells also displayed nuclear localization of FOXO3a in the presence of glutamate (examined for 0 h, 1.5 h, 3 h and 6 h) which was inhibited in the presence of roscovitine (Fig. 3C,D). These results were further confirmed using Cdk5 shRNA, which confirmed complete inhibition of FOXO3a nuclear translocation in the presence of glutamate (Fig. 3E,F). Finally, we also conducted nuclear and cytosolic fractionation, which also validated that Cdk5 is responsible for FOXO3a migration to the nucleus in glutamate-treated cells (Fig. 3G). These findings confirmed that wild-type HA-tagged FOXO3a behaves similarly to endogenous Foxo3 and shows identical subcellular localization in untreated and glutamate-treated HT22 cells.

We next generated a HT22 cell line expressing the phosphorylation-resistant FOXO3a mutant (4A-FOXO3a-HT22) and exposed these cells to glutamate for varying periods. Similar to wild-type FOXO3a-HT22 cells, a robust nuclear localization of Cdk5 was observed in these cells upon glutamate treatment (Fig. 4A,B). However, in contrast to wild-type FOXO3a, which migrated to the nucleus following glutamate exposure, 4A-FOXO3a remained in the cytoplasm even after 6 h of glutamate treatment (Fig. 4A,C). Cytoplasmic and nuclear fractionation of untreated and glutamate-treated HT22 cells further confirmed this finding (Fig. 4D). Taken together, these data show that nuclear translocation of Foxo3 depends on Cdk5-mediated phosphorylation and is independent of nuclear envelope dispersion triggered by Cdk5 (Chang et al., 2011).

Cdk5-mediated phosphorylation increases Foxo3 levels in glutamate-treated HT22 cells

We next investigated whether Foxo3 translocation to the nucleus affects its protein levels. Neurotrophic factors such as brain-derived neurotrophic factor (BDNF) and nerve growth factor activate Akt, which downregulates FOXO protein levels in the cytoplasm (Gan et al., 2005), suggesting that nuclear translocation of Foxo3 might increase its protein levels. To test this hypothesis, we investigated total Foxo3 levels (cytoplasmic and nuclear) in HT22 cells treated with glutamate for 6 h, 12 h and 24 h. Glutamate treatment for 12 h resulted in a significant increase in Foxo3 levels, which then decreased significantly in 24 h (Fig. 4E,F). This result was not surprising as a large percentage of cells die in 24 h following glutamate treatment (Sun et al., 2008a,b). Thus, glutamate treatment not only results in Foxo3 translocation to the nucleus, it also increases the levels of Foxo3. Fig. 4F displays average Foxo3 levels upon glutamate treatment from three independent experiments.

To determine whether this increase in Foxo3 levels is Cdk5 dependent, we examined Foxo3 levels in HT22 cells exposed to glutamate for 12 h in the presence or absence of Cdk5 shRNA or roscovitine. Glutamate treatment resulted in a significant increase in Foxo3 levels, which was inhibited by Cdk5 inhibition or Cdk5 depletion (Fig. 4G). To examine the contribution of Cdk5-mediated phosphorylation of Foxo3 in this process, we exposed FOXO3a-HT22 and 4A-FOXO3a-HT22 cells to glutamate for 12 h in the presence or absence of either roscovitine or Cdk5 shRNA. In glutamate-treated wild-type FOXO3a-HT22 cells, Foxo3 levels increased in a Cdk5-dependent manner (Fig. 4H), whereas 4A-FOXO3a-HT22 cells showed a minimal increase in Foxo3 levels, which remained largely unaffected by Cdk5 knockdown or inhibition (Fig. 4I). Taken together, these results show that Cdk5 increases Foxo3 levels in neurotoxin-exposed neuronal cells by direct phosphorylation.

Cdk5 activates Foxo3 transcriptional activity

As our results revealed that Cdk5 promotes Foxo3 translocation to the nucleus in glutamate-treated cells, we hypothesized that Cdk5 might modulate Foxo3 transcriptional activity. We initially measured Foxo3 transcriptional activity in control and p25-transfected HT22 cells using a luciferase assay, which revealed an ∼4-fold increase in Foxo3 transcriptional activity, suggesting that in addition to its nuclear translocation, Cdk5 also activates Foxo3 transcriptional activity (Fig. 5A). To further examine Foxo3 transcriptional activity under neurotoxic conditions, we treated HT22 cells with glutamate for varying periods, which revealed a more than 4-fold time-dependent increase in Foxo3 transcriptional activity after 6 h of treatment. Most importantly, when Cdk5 was inhibited using roscovitine or knocked down, the increase in Foxo3 transcriptional activity was largely inhibited suggesting that Foxo3 is predominantly regulated by Cdk5 under neurotoxic conditions (Fig. 5B).

Activation of Foxo3 is neurotoxic in glutamate-treated cells

Foxo3 activation can lead to either cell survival or cell death depending upon the cellular context and insult. Therefore, we

Journal of Cell Science (2016) 129, 1815-1830 doi:10.1242/jcs.185009

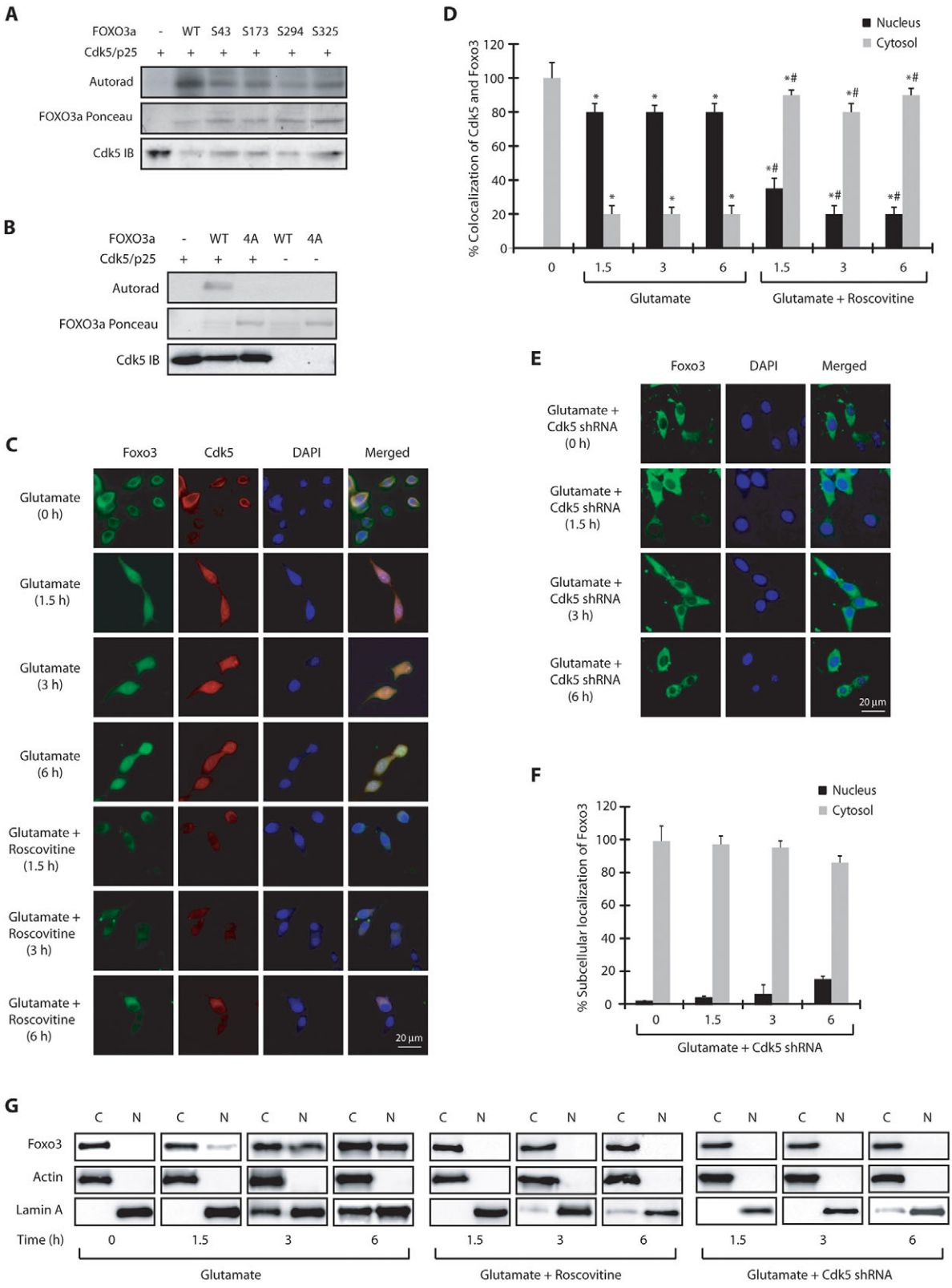

Fig. 3. Cdk5 directly phosphorylates FOXO3a at multiple sites. (A) The Cdk5–p25 complex (Cdk5/p25) phosphorylates FOXO3a at S43, S173, S294 and S325 (human numbering). Recombinant 6×-His-tagged wild-type and FOXO3a mutants were subjected to a kinase assay with Cdk5–p25. (B) Cdk5 does not phosphorylate the quadruple 4A-FOXO3a mutant. (C) Glutamate stimulates nuclear translocation of Cdk5 and FOXO3a in FOXO3a-HT22 cells. FOXO3a-HT22 cells were treated with glutamate for 0–6 h, followed by immunostaining. Representative pictures are shown. (D) The percentage of cells showing nuclear translocation of Cdk5 and Foxo3. *P<0.01, compared with untreated HT22 cells; $^{\#}P$<0.01, compared with corresponding glutamate-treated HT22 cells (Student's t-test). (E) Cdk5-shRNA-infected HT22 cells were treated with glutamate (0–6 h). Representative pictures are shown. (F) The percentage of cells showing nuclear translocation of Foxo3. (G) Subcellular fractionation of Foxo3 in glutamate-treated FOXO3a-HT22 cells in the absence or presence of roscovitine or Cdk5 shRNA. Actin is the cytoplasmic marker and lamin A is the nuclear marker. N, nuclear fraction; C, cytoplasmic fraction. Graphical results are mean±s.e.m. Each experiment was repeated at least three independent times.

Journal of Cell Science

Journal of Cell Science (2016) 129, 1815-1830 doi:10.1242/jcs.185009

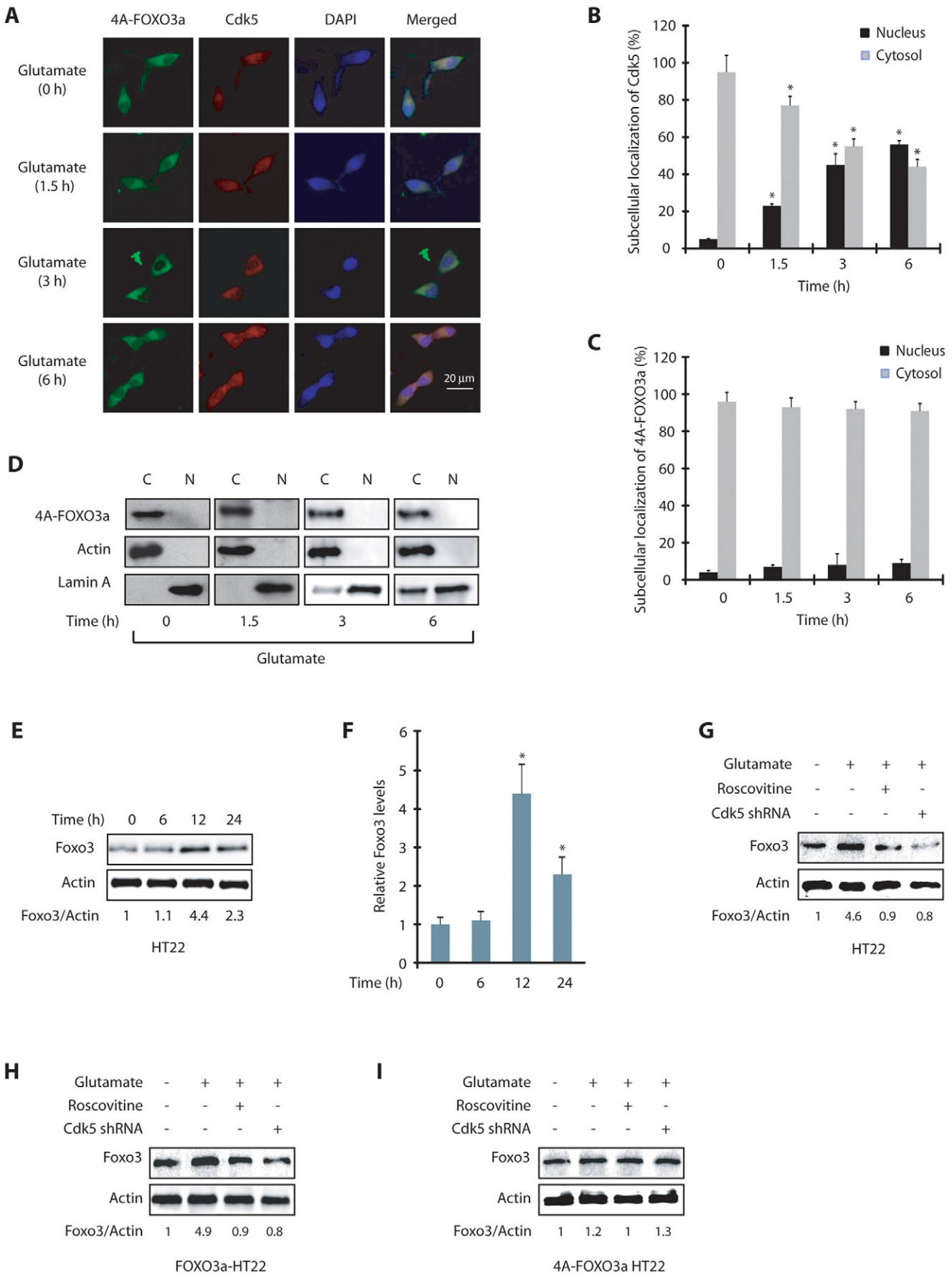

Fig. 4. See next page for legend.

Journal of Cell Science (2016) 129, 1815-1830 doi:10.1242/jcs.185009

Fig. 4. Foxo3 translocation to the nucleus is phosphorylation-dependent. (A) 4A-FOXO3a-HT22 cells were treated with glutamate for 0–6 h, followed by immunostaining with anti-HA antibody (clone #12CA5). Representative pictures are shown. (B) The percentage of cells showing nuclear translocation of Cdk5. *P<0.01, compared with untreated HT22 cells (Student's t-test). (C) The percentage of cells showing nuclear translocation of 4A-FOXO3a. (D) Subcellular fractionation of 4A-FOXO3a in glutamate-treated 4A-FOXO3a-HT22 cells. 4A-FOXO3a was visualized using anti-HA antibody. Actin is the cytoplasmic marker and lamin A is the nuclear marker. N, nuclear fraction; C, cytoplasmic fraction. (E) HT22 cells were treated with glutamate for 0–24 h and the total levels of Foxo3 analyzed. (F) Average relative ratios of Foxo3 band intensities to actin band intensities upon glutamate treatment are shown from three independent experiments. *P<0.01, compared with untreated HT22 cells (Student's t-test). (G) HT22 cells were treated with glutamate for 12 h, in the presence and absence of roscovitine or Cdk5 shRNA and then the total levels of Foxo3 were analyzed. (H) FOXO3a-HT22 cells were treated similarly to in G and total levels of Foxo3 analyzed. (I) 4A-FOXO3a-HT22 cells were treated similarly to in G and the Foxo3 levels analyzed. Graphical results are mean±s.e.m. Each experiment was repeated at least three independent times.

investigated whether activation of Foxo3 was neuroprotective or neurotoxic in glutamate-treated HT22 cells. HT22 cells exposed to glutamate for 24 h exhibited an ∼60% loss in cell viability, which was fully inhibited in the absence of Cdk5 (Fig. 5C), which is consistent with previous reports highlighting a key role of Cdk5 in glutamate-induced neurotoxicity (Sun et al., 2008a,b). Interestingly, Cdk5 inhibition using roscovitine was only partially neuroprotective, in contrast to Cdk5 shRNA, which was similar to our previous results (Sun et al., 2008a). This partial protection was presumably because roscovitine also inhibits Cdk1 and Cdk2 (Meijer et al., 1997), both of which are crucial for a normal cell cycle in HT22 cells (Fig. 5C). Importantly, Foxo3 depletion significantly protected glutamate-treated HT22 cells, suggesting that Foxo3 activation upon glutamate stimulation is, in fact, toxic to the cells.

Downstream effects of Foxo3 in glutamate-exposed cells: Bim, FasL, MnSOD and amyloid precursor protein (APP)

The downstream molecular alterations due to Foxo3 activation were next examined in a time-dependent manner in these cells following glutamate treatment. As more than 50% of the glutamate-exposed cells die in 24 h (Fig. 5C, column 2), we chose both early and late time points to monitor the activation of various genes using the corresponding luciferase plasmids. Notably, Foxo3 was found to be activated at as early as 1.5 h after glutamate treatment, and continued to increase with time (Fig. 5B).

As Foxo3 is known to regulate Bim (also known as BCL2L11) and FasL (also known as FASLG) leading to apoptosis, we transiently expressed Bim and FasL promoter luciferase plasmids into HT22 cells and monitored their potential activation following glutamate stimulation for 0 h, 6 h, 12 h, 18 h and 24 h. No activation of Bim promoter was observed at 6 h, but after 12 h of glutamate treatment, an ∼4-fold activation of Bim was observed that steadily increased up to 24 h (6-fold). Cdk5 depletion or Foxo3 depletion largely inhibited the increase in Bim promoter activity at all time points, suggesting that Bim activation is predominantly mediated by Cdk5 and Foxo3 (Fig. 5D). Interestingly, similar to our MTT assay results, inhibition of Cdk5 with roscovitine only partially reduced Bim levels, suggesting that concurrent inhibition of other Cdks by roscovitine in HT22 cells might promote cell toxicity. FasL was also upregulated upon glutamate treatment and displayed similar kinetics to that of Bim. FasL upregulation was significantly inhibited independently by both Cdk5 and Foxo3 depletion, suggesting that it is downstream of Cdk5 and Foxo3 (Fig. 5E).

In addition to the pro-apoptotic genes Bim and FasL, we also monitored a potential effect on the promoter activity of manganese superoxide dismutase (MnSOD, also known as SOD2) despite the fact that Foxo3 appeared to support cell death (Fig. 5C). Foxo3 is known to regulate MnSOD upon oxidative stress (Kops et al., 2002). We hypothesized that upon initial glutamate treatment, the cells might strive to survive and thus might upregulate MnSOD, but later (after a point of no return) upregulate other cell death genes. Our data indeed revealed that MnSOD promoter is activated after 6 h of treatment (∼1.5-fold), which further increased to more than 2.5-fold in 12 h (Fig. 5F). Both of these activation events were Cdk5 and Foxo3-dependent. Furthermore, MnSOD promoter activity returned to basal levels at 18 h and 24 h following glutamate treatment. We have previously shown an increase in ROS levels in glutamate-treated HT22 cells (∼1.5–2-fold in 4 h which increased to 2.5-fold by 8–12 h) (Sun et al., 2008b, 2009; Chang et al., 2010), suggesting that an increase in ROS levels triggers the activation of Foxo3 to upregulate MnSOD initially. However, increasingly neurotoxic conditions then favor cell death and lead to the upregulation of the pro-apoptotic genes Bim and FasL.

We also examined a potential effect of Foxo3 on amyloid precursor protein (APP) promoter activity. Although Foxo3 has not been identified as an upstream regulator of APP processing, a recent study identified Foxo3 as a downstream target of APP, which induces APP intracellular domain (AICD)-induced death in neuronal and non-neuronal tissues (Wang et al., 2014). Glutamate treatment led to an ∼2-fold increase in APP promoter activity in 12 h, which gradually increased to 2.5-fold by 24 h (Fig. 5G). Depletion of either Cdk5 or Foxo3 using corresponding shRNAs significantly inhibited the activation of the APP promoter, suggesting that Foxo3 acts as an upstream regulator of the expression of APP (Fig. 5G).

We then chose one cell death gene (Bim) and one neuroprotective gene (MnSOD) to analyze their protein levels in glutamate-exposed HT22 cells to confirm the activation of their corresponding promoters (Fig. 5D and F, respectively). As noted above, Bim activation continued increasing until 24 h, whereas the MnSOD promoter showed maximal activation after 12 h, and then decreased significantly by 24 h (Fig. 5D and F, respectively). These findings prompted us to choose the 0 h, 18 h and 24 h time points following glutamate treatment to analyze the levels of Bim and 0 h, 12 h, 18 h and 24 h for MnSOD in HT22 cells.

Consistent with the results obtained using the promoter assay, Bim levels increased >8-fold by 18 h, and >9-fold by 24 h (Fig. 5H). Importantly, Cdk5 knockdown or Foxo3 knockdown prevented this increase, underscoring the key role of Cdk5 and Foxo3 in promoting cell death through Bim upregulation (Fig. 5I). In contrast to Bim levels in glutamate-treated HT22 cells, MnSOD levels increased by ∼4-fold after 12 h and 18 h, but decreased below basal levels by 24 h, further confirming that MnSOD expression is downregulated when the cells are committed to die (Fig. 5J). Furthermore, we observed that, similar to Bim, MnSOD was also upregulated in a Cdk5- and Foxo3-dependent manner (Fig. 5K). Collectively, these data confirm that Cdk5 and Foxo3 regulate transcriptional activation of Bim, FasL, MnSOD and APP, as depletion of either using corresponding shRNA inhibits their activation.

Consequences of Cdk5-mediated phosphorylation of Foxo3a

To uncover the significance of Cdk5-mediated phosphorylation of Foxo3 in these processes, we next compared the promoter activities of Foxo3, Bim, FasL, MnSOD and APP in HT22, FOXO3a-HT22 and 4A-FOXO3a-HT22 cells.

Journal of Cell Science (2016) 129, 1815-1830 doi:10.1242/jcs.185009

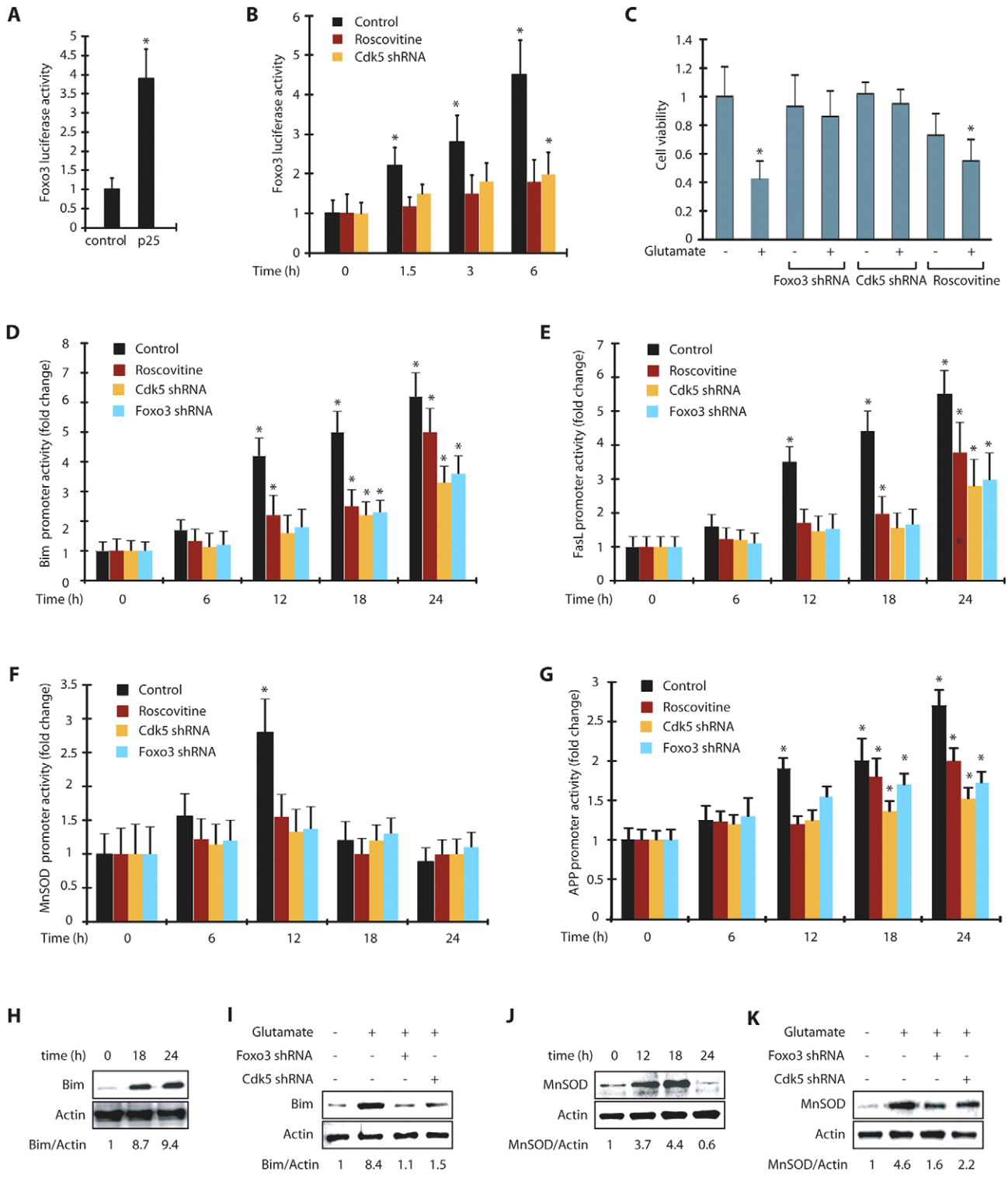

Fig. 5. Cdk5-mediated Foxo3 activation increases the promoter activities of Bim, FasL, MnSOD and APP. (A) Foxo3 promoter activity was determined in vector and p25-expressing cells **P*<0.01, compared with untreated HT22 cells (Student's *t*-test). (B) Foxo3 promoter activity was determined in HT22 cells upon glutamate treatment with or without roscovitine and Cdk5 shRNA. **P*<0.01, compared with untreated HT22 cells (Student's *t*-test). (C) Scrambled-shRNA-infected, Cdk5-shRNA- or Foxo3-shRNA-infected or roscovitine-exposed HT22 cells were treated with glutamate for 24 h. Cell viability was examined using an MTT assay. **P*<0.01, compared with untreated HT22 cells (Student's *t*-test). (D) Bim promoter activity was determined in HT22 cells upon glutamate treatment. (E) FasL promoter activity was determined in HT22 cells upon glutamate treatment. **P*<0.01, compared with untreated HT22 cells (Student's *t*-test). (F) MnSOD promoter activity was determined in HT22 cells upon glutamate treatment. **P*<0.01, compared with untreated HT22 cells (Student's *t*-test). (G) APP promoter activity was determined in HT22 cells upon glutamate treatment. **P*<0.01, compared with untreated HT22 cells (Student's *t*-test). (H) HT22 cells were treated with glutamate for 0–24 h and Bim levels analyzed. (I) HT22 cells were treated with glutamate for 18 h with or without Cdk5 shRNA or Foxo3 shRNA. The total level of Bim was analyzed. (J) HT22 cells were treated with glutamate similarly and MnSOD levels analyzed. (K) HT22 cells were treated with glutamate, with and without Foxo3 shRNA or Cdk5 shRNA, and MnSOD levels analyzed. Graphical results are mean±s.e.m. Each experiment was repeated at least three independent times.

Journal of Cell Science

Journal of Cell Science (2016) 129, 1815-1830 doi:10.1242/jcs.185009

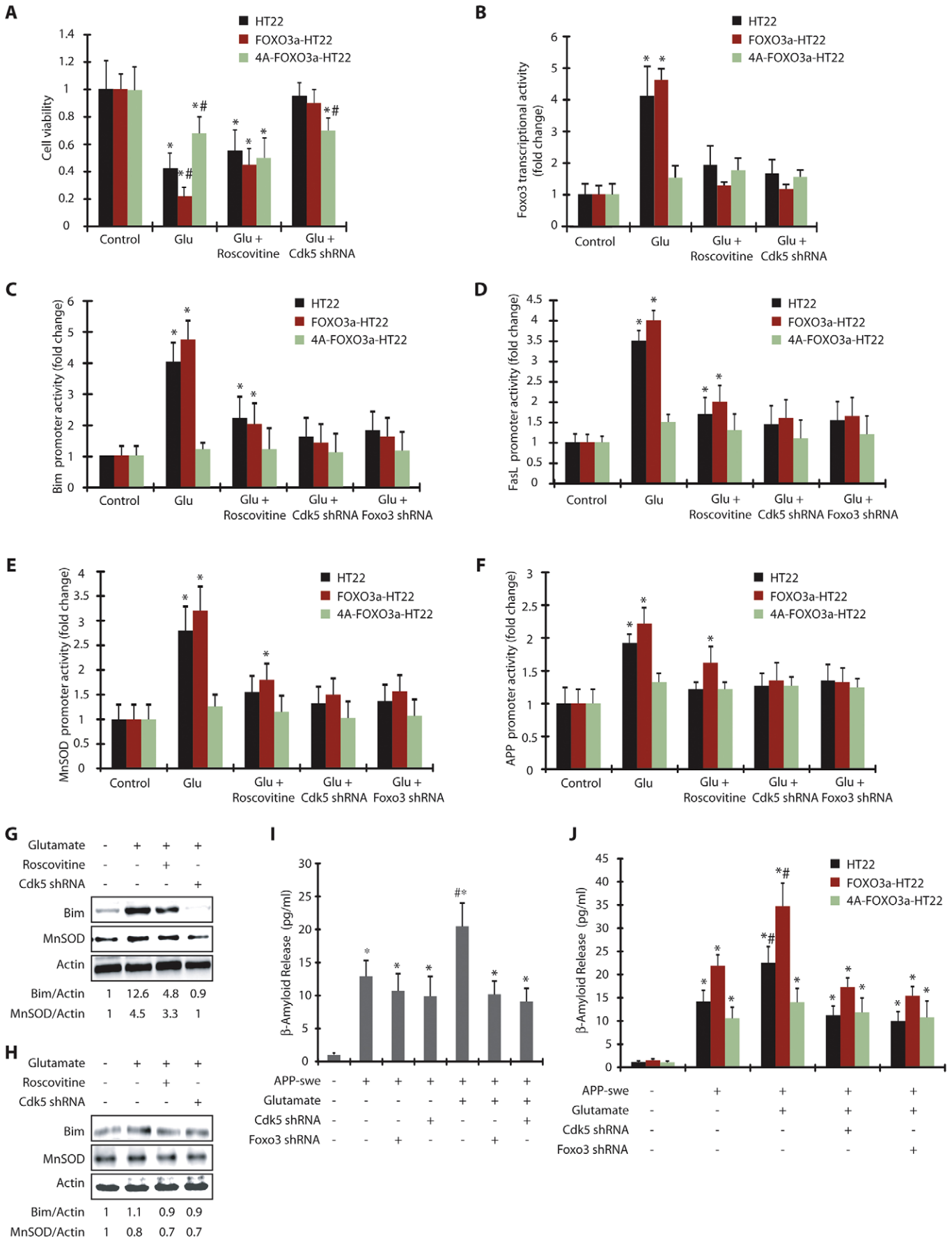

Fig. 6. See next page for legend.

Journal of Cell Science (2016) 129, 1815-1830 doi:10.1242/jcs.185009

Fig. 6. Cdk5-mediated activation of Foxo3 and its downstream genes are phosphorylation-dependent. (A) HT22, FOXO3a-HT22 and 4A-FOXO3a-HT22 cells were treated with glutamate, roscovitine and Cdk5 shRNA and cell viability tested by using an MTT assay. **P*<0.01, compared with untreated HT22 cells; #*P*<0.01, compared with glutamate-treated HT22 cells (Student's *t*-test). (B) HT22, FOXO3a-HT22 and 4A-FOXO3a-HT22 cells transfected with pGL3-based Foxo3 promoter plasmid were treated with glutamate in the presence or absence of roscovitine or Cdk5 shRNA and the promoter activity measured. **P*<0.01, compared with untreated HT22 cells (Student's *t*-test). (C) Bim promoter activity was measured in glutamate, roscovitine, Foxo3 shRNA and Cdk5 shRNA-treated HT22, FOXO3a-HT22 and 4A-FOXO3a-HT22 cells. **P*<0.01, compared with untreated HT22 cells. (D) FasL promoter activity was measured in glutamate, roscovitine, Foxo3-shRNA- and Cdk5-shRNA-treated HT22, FOXO3a-HT22 and 4A-FOXO3a-HT22 cells. **P*<0.01, compared with untreated HT22 cells (Student's *t*-test). (E) HT22, FOXO3a-HT22 and 4A-FOXO3a-HT22 cells were transfected with pGL3-based MnSOD promoter, followed by various treatments and the promoter activity measured. **P*<0.01, compared with untreated HT22 cells (Student's *t*-test). (F) APP promoter activity was measured in glutamate, roscovitine, Foxo3 shRNA and Cdk5-shRNA-treated cells **P*<0.01, compared with untreated cells (Student's *t*-test). (G) FOXO3a-HT22 cells pretreated with roscovitine or Cdk5 shRNA were treated with glutamate for 18 h. The total levels of Bim or MnSOD were analyzed. (H) 4A-FOXO3a-HT22 cells pretreated with roscovitine or Cdk5 shRNA were treated with glutamate (18 h). The total levels of Bim or MnSOD were analyzed. (I) APP-swe plasmid was transfected into HT22 cells for 40 h, followed by 18 h of glutamate treatment. Cdk5 shRNA or Foxo3 shRNA were added 30 h prior to glutamate treatment. β-amyloid (1-42) released into the medium was measured as described in the Materials and Methods. **P*<0.01, compared with untreated HT22 cells; #*P*<0.01, compared with glutamate-treated HT22 cells (Student's *t*-test). (J) APP-swe was transfected into HT22, FOXO3a-HT22 and 4A-FOXO3a-HT22 cells, followed by various treatments. β-amyloid(1–42) released into the medium was measured. Graphical results are mean±s.e.m. Each experiment was repeated at least three independent times.

As Foxo3 depletion largely prevented neurotoxicity in glutamate-treated HT22 cells (Fig. 5C), we initially compared the consequences of glutamate exposure in wild-type and 4A-FOXO3a-HT22 cells. Although expression of wild-type Foxo3 rendered HT22 cells more sensitive to glutamate-induced toxicity, expression of 4A-FOXO3a conferred substantial resistance, suggesting that Cdk5-mediated phosphorylation of Foxo3 is neurotoxic in HT22 cells (Fig. 6A).

These results also suggest that 4A-Foxo3 acts as a dominant-negative modulator, and might affect endogenous Foxo3 activation. Thus, we measured the promoter activity of Foxo3 in untreated and glutamate-treated HT22, FOXO3a-HT22 and 4A-FOXO3a-HT22 cells. As expected, both HT22 cells and HT22 cells expressing wild-type FOXO3a showed significant activation, which was prevented in the presence of either Cdk5 shRNA or roscovitine (Fig. 6B). In contrast, expression of 4A-FOXO3a showed minimal activation upon glutamate stimulation, thereby confirming that Cdk5-mediated phosphorylation causes Foxo3 activation.

We also analyzed Bim, FasL, MnSOD and APP promoter activities in HT22, FOXO3a-HT22 and 4A-FOXO3a-HT22 cells exposed to glutamate. As 12 h of glutamate treatment revealed a substantial increase in Bim, FasL, MnSOD and APP promoter activities (Fig. 5D–G), this time point was chosen. HT22 and FOXO3a-HT22 showed substantial activation of Bim, FasL, MnSOD and APP promoters, all of which were Cdk5 dependent (Fig. 6C–F). By contrast, 4A-FOXO3a-HT22 cells offered significant resistance and prevented the activation of Bim, FasL, MnSOD and APP promoters when exposed to glutamate (Fig. 6C–F). Taken together, these findings strongly support that Cdk5-mediated phosphorylation of Foxo3 is a key mechanism in glutamate-induced upregulation of MnSOD and other cell death genes.

These results were further validated by analyzing Bim and MnSOD protein levels in glutamate-treated FOXO3a-HT22 cells with and without Cdk5 inhibition or depletion. Bim level increased >12-fold after 18 h of glutamate treatment, which was fully prevented by Cdk5 knockdown (Fig. 6G). Interestingly, Cdk5 inhibition using roscovitine partially inhibited Bim level, presumably due to the inhibition of other Cdks in HT22 cells, causing toxicity. Similarly, MnSOD level also increased in glutamate-treated HT22 cells, which was partially inhibited by roscovitine and fully inhibited by Cdk5 depletion (Fig. 6G). Conversely, both Bim and MnSOD levels remained unaffected in glutamate-treated 4A-FOXO3a-HT22 cells, confirming that Cdk5-mediated phosphorylation of Foxo3 is responsible for the upregulation of Bim and MnSOD levels (Fig. 6H).

Cdk5-mediated Foxo3 regulation increases Aβ(1–42) levels

As HT22 cells do not produce detectable levels of Aβ(1–42) upon glutamate stimulation, we transfected them with Swedish APP (Swedish mutation K595N/M596L of APP, APP-swe) plasmid, which increases abnormal cleavage of cellular APP by β-secretase, leading to NFT formation in early-onset Alzheimer's disease (Haass et al., 1995). Ectopic expression of APP-swe increased basal levels of secreted Aβ(1–42) (~13 pg/ml) (Fig. 6I). Importantly, depletion of Foxo3 or Cdk5 exhibited no change in secreted Aβ(1–42) levels, suggesting that this basal secretion is independent of Cdk5 and Foxo3 regulation. When these cells were treated with glutamate (18 h), there was a significant increase in Aβ(1–42) secretion, which was prevented when either Cdk5 or Foxo3 was depleted (Fig. 6I). Collectively, these data show that Cdk5 not only regulates reactive oxygen species (ROS) scavenging and cell death genes through Foxo3 in glutamate-stressed cells, it also promotes neurotoxic Aβ (1–42) processing after Foxo3 activation, thereby contributing to two hallmarks of Alzheimer's disease.

To further examine the role of Foxo3 phosphorylation in Aβ(1–42) processing, we ectopically expressed APP-swe in HT22, FOXO3a-HT22 and 4A-FOXO3a-HT22 cells, which resulted in increased secretion of Aβ(1–42) in all three cell types (Fig. 6J). Importantly, glutamate stimulation increased Aβ(1–42) levels in HT22 and FOXO3a-HT22 cells, which was prevented by knocking down Foxo3 or Cdk5. In contrast, 4A-FOXO3a-HT22 cells did not respond to glutamate-induced toxicity, thereby highlighting a crucial role of both Cdk5 and Foxo3 in promoting aberrant Aβ processing.

Foxo3 signaling in mature primary cortical neurons

To determine a potential role of Cdk5 in regulating Foxo3 signaling under more pathologically relevant conditions, we chose 100 μM glutamate as the stimulus to induce excitotoxicity in mature mouse primary cortical neurons (Hosie et al., 2012). We initially analyzed whether glutamate-treatment affects the subcellular localization of Foxo3 and whether it was Cdk5 dependent. Similar to the results obtained in glutamate-treated HT22 cells, mouse primary cortical neurons exposed to glutamate led to a robust increase in the nuclear translocation of both Cdk5 and Foxo3, which was inhibited by roscovitine or Cdk5 depletion (Fig. 7A,B). Importantly, Cdk5 inhibition or depletion also resulted in significant shrinkage of neurites and axon, which is consistent with previous findings highlighting a key role of Cdk5 in neuronal differentiation in primary cortical neurons (Fig. 7A,B) (Nikolic et al., 1996).

Furthermore, glutamate stimulation also resulted in substantial activation of Foxo3, Bim, FasL, MnSOD and APP promoter activities (Fig. 7C–G). Depletion of either Cdk5 or Foxo3 largely inhibited their activation, suggesting that these activations were both

Journal of Cell Science

Journal of Cell Science (2016) 129, 1815-1830 doi:10.1242/jcs.185009

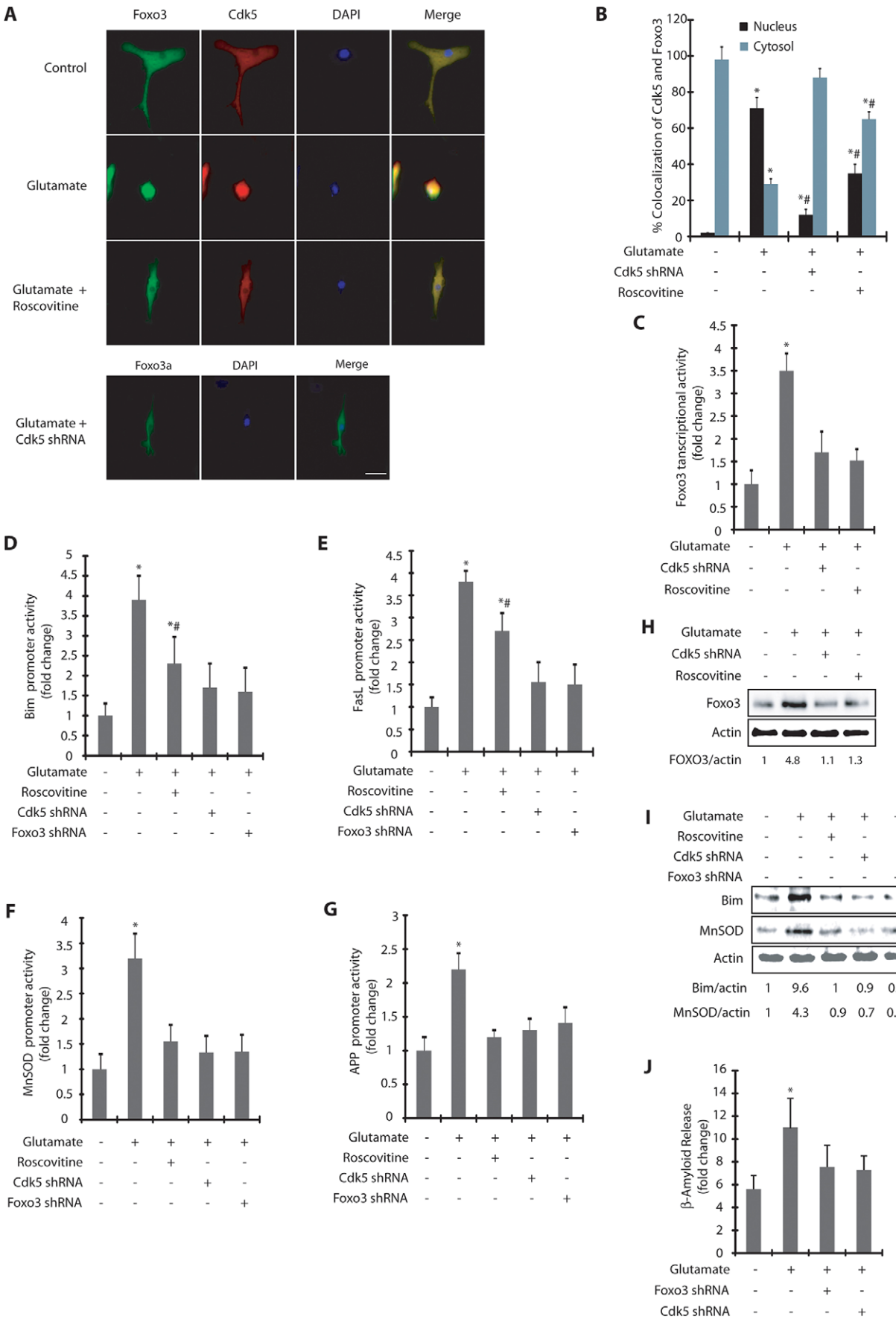

Fig. 7. See next page for legend.

Journal of Cell Science (2016) 129, 1815-1830 doi:10.1242/jcs.185009

Fig. 7. Foxo3 signaling in primary neurons. (A) Primary cortical neurons were treated with glutamate (100 µM) for 6 h in the presence or absence of roscovitine and Cdk5 shRNA, followed by immunostaining. Scale bar: 20 µm. (B) The percentage of cells showing nuclear translocation of Cdk5 and Foxo3. **P*<0.01, compared with untreated HT22 cells; #*P*<0.01, compared with glutamate-treated HT22 cells (Student's *t*-test). (C) Foxo3 promoter activity was determined as described in the Materials and Methods. **P*<0.01, compared with untreated HT22 cells (Student's *t*-test). (D–G) Bim, FasL, MnSOD and APP promoter activities were measured upon various treatments. **P*<0.01, compared with untreated primary cortical neurons (Student's *t*-test); #*P*<0.01, compared with glutamate-treated HT22 cells (Student's t-test). (H) Foxo3 levels were analyzed upon glutamate (12 h), roscovitine and Cdk5 shRNA treatments. (I) Bim or MnSOD levels were analyzed upon glutamate, roscovitine, Foxo3 shRNA and Cdk5 shRNA treatments for 12 h. (J) Primary cortical neurons cells were treated with 100 µM glutamate for 18 h. Cdk5 shRNA or Foxo3 shRNA were added 30 h prior to glutamate treatment. Aβ(1–42) released into the medium was measured with an ELISA kit. **P*<0.01, compared with untreated neurons (Student's *t*-test). Graphical results are mean±s.e.m. Each experiment was repeated at least three independent times.

Cdk5 and Foxo3 dependent. Finally, we confirmed these findings by analyzing Foxo3, Bim and MnSOD levels in untreated and glutamate-exposed primary neurons (12 h). Glutamate treatment led to a ∼5-fold increase in Foxo3 levels, which was prevented in the presence of Cdk5 shRNA or roscovitine (Fig. 7H). Similarly, Bim showed a >9-fold increase upon glutamate exposure which was both dependent on both Cdk5 and Foxo3 (Fig. 7I). Likewise, MnSOD was increased more than 4-fold by 12 h, which was prevented if either Cdk5 or Foxo3 was depleted. Collectively, these results confirm that, similar to HT22 cells, glutamate stimulation in primary cortical neurons also triggers Cdk5-dependent Foxo3 nuclear translocation and activation, leading to an increase in Bim, FasL, MnSOD and APP promoter activities.

We next investigated whether Foxo3 regulates Aβ(1–42) levels upon excitotoxicity in primary cortical neurons. Unlike HT22 cells, which required ectopic expression of APP-swe to elicit the secretion of Aβ(1–42), in primary cortical neurons, excitotoxicity triggered the release of Aβ(1–42), which was both Cdk5 and Foxo3 dependent (Fig. 7J). Thus, Cdk5-mediated regulation of Foxo3 and its downstream consequences were found to be similar in both HT22 cells and primary cortical neurons, which underscores the relevance of this pathway in Alzheimer's disease pathogenesis.

As Foxo3 activation is linked both to cell survival and cell death, we investigated the consequences of Foxo3 activation in glutamate-induced neurotoxicity in primary cortical neurons. Glutamate exposure (100 µM) for 24 h led to a >60% loss of cell viability in primary cortical neurons, which was fully rescued in the presence of either Cdk5 shRNA or Foxo3 shRNA, thereby highlighting a crucial neurotoxic role of Foxo3 in primary cortical neurons upon neurotoxic insults (Fig. 8A). Roscovitine treatment partially prevented loss of cell viability, consistent with the results obtained in HT22 cells (Fig. 5C).

The role of Cdk5 in inducing synaptic toxicity was next examined by analyzing the distribution of PSD95 (also known as DLG4), a postsynaptic protein in primary cortical neurons exposed to cellular treatments. Our data showed that the cortical neuron immunostained with antibodies against PSD95 (green) and MAP2 (a neuronal protein, red) displayed the intact neurites, but glutamate treatment caused severe neuritic shrinkage as well as lower PSD95 levels, which is consistent with previous findings (Fig. 8B). Inhibition or ablation of Cdk5 prevented PSD95 downregulation, highlighting a role of deregulated Cdk5 in synaptic toxicity. As noted before, Cdk5 inhibition or ablation also led to the retraction of neurites due to its key role in neuronal differentiation.

Foxo3 levels increase in the p25 transgenic mouse model of Alzheimer's disease upon p25 induction

The contribution of active Foxo3 towards neurotoxic Aβ formation and neuronal death, the two hallmarks of Alzheimer's disease, prompted us to investigate Cdk5–Foxo3 regulation in a well-established model of Alzheimer's disease *in vivo*. To test whether the alteration of Foxo3 levels could be induced by Cdk5 *in vivo*, we examined the effect of Cdk5 activation on Foxo3 in forebrain-neuron-specific p25-inducible transgenic mice (Cruz et al., 2003). Using immunocytochemistry analysis, we found a significant increase in Foxo3 levels and nuclear localization after a 2-week induction of p25 in hippocampal neurons compared to control (Fig. 8C). We also observed robust astrocytosis (using GFAP staining) and induction of markers of cell cycle re-entry (PCNA) in the same area, which are consistent with previously published findings (Kim et al., 2008), and indicates Foxo3 is correlated with other early pathological changes induced by p25 overexpression. Thus, these data strongly confirm the results obtained from HT22 and primary neurons, and suggest that the activation of Cdk5 in p25-inducible mice induces the expression and nuclear localization of Foxo3 levels. Given that neuronal cell death is initiated after 8 weeks of induction in these p25-inducible transgenic mice (Cruz et al., 2003), our data also indicate that the alteration of Foxo3 levels is an early event following Cdk5 activation and precedes neuronal cell death in this mouse model, which is also consistent with our findings with the neuronal cell culture models.

DISCUSSION

FOXO3a is highly expressed in human brain, specifically in those areas that are highly vulnerable to neurodegeneration in Alzheimer's disease (Hoekman et al., 2006). We identified this isoform as a direct Cdk5 substrate by our chemical genetic screen using mouse brain lysates. FOXOs regulate diverse physiological functions including the stress response, cell cycle arrest, metabolism, longevity and apoptosis (Calnan and Brunet, 2008). The transcriptional activity of FOXOs is regulated by their subcellular localization. FOXOs are inactive in the cytoplasm and active in the nucleus. Growth and survival signals activate Akt, which phosphorylates FOXO3a at three conserved sites, sequestering it in the cytoplasm and rendering it inactive (Zhu et al., 2004). In contrast, stress signals such as oxidative stress, ischemia and DNA damage, prompt nuclear localization of FOXOs, rendering them transcriptionally active.

A few studies have addressed FOXO signaling in neurons and its relevance to Alzheimer's disease. The most important link between FOXOs and Alzheimer's disease is oxidative stress. Oxidative stress is one of the earliest triggers in Alzheimer's disease pathology. FOXOs are activated in response to oxidative stress, conferring either stress resistance or cell death depending on the cell type. In H_2O_2-treated DL23 cells, FOXO3a cleans up ROS by upregulating MnSOD (Kops et al., 2002). In contrast, in mouse cerebellar granule neurons, H_2O_2-induced Foxo3 activation promotes cell death (Dávila and Torres-Aleman, 2008; Peng et al., 2015). Similarly, in primary neurons, oxidative-stress-induced Foxo3 activation causes apoptotic cell death (Wang et al., 2013). Iron-induced oxidative stress in HT22 cells activates Akt, which blocks Foxo3 activation promoting neuronal survival (Uranga et al., 2013). A recent report further showed that Aβ treatment in primary cortical neurons leads to MST1-mediated phosphorylation of Foxo3, which induces its nuclear translocation and eventual cell death (Sanphui and Biswas, 2013). Despite this significant role of FOXOs under neurotoxic conditions, regulation of FOXOs and their

Journal of Cell Science (2016) 129, 1815-1830 doi:10.1242/jcs.185009

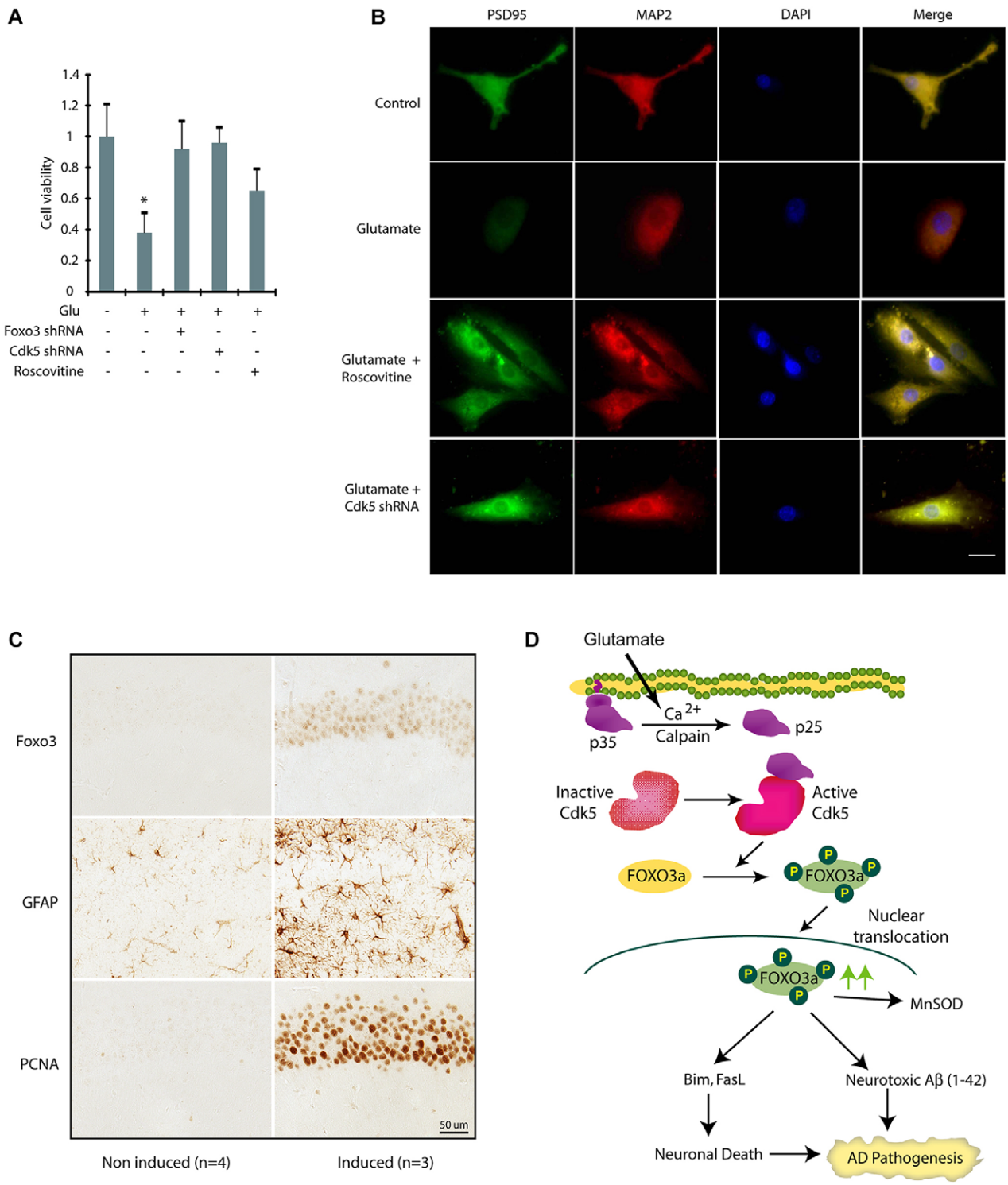

Fig. 8. Cdk5 deregulation due to p25 expression promotes increased expression and nuclear localization of Foxo3 *in vivo*. (A) Inhibition and ablation of Cdk5 inhibits neurotoxicity in primary cortical neurons. Cdk5-shRNA- or Foxo3-shRNA-infected primary neurons (30 h) were treated with glutamate (24 h). Cell viability was tested by an MTT assay. **P*<0.01, compared with untreated neurons (Student's *t*-test). (B) Primary cortical neurons pre-treated with roscovitine or Cdk5 shRNA were treated with glutamate for 12 h, followed by immunostaining with PSD95 or MAP2 and DAPI. Representative pictures are shown. Scale bar: 20 µm. (C) The increased expression and nuclear localization of Foxo3 in hippocampal neurons in p25 transgenic mice. After the induction of p25 for 2 weeks, the level of Foxo3 in nuclei of the hippocampal CA1 neurons is significantly increased (*P*<0.05, Student's *t*-test). Astrocytosis (GFAP) and cell cycle re-entry (PCNA) are also highly induced in the same area which is consistent with previously published findings and indicates Foxo3 is correlated with other early pathological changes induced by p25 overexpression. (D) Our model showing that Cdk5-mediated Foxo3 activation contributes to two hallmarks of Alzheimer's disease.

consequences remain incompletely understood in Alzheimer's disease pathogenesis. Similarly, the role of FOXOs in glutamate-mediated neurotoxicity is largely unknown.

In the present study, we identified Cdk5 as a major regulator of Foxo3 signaling under neurotoxic conditions. Cdk5 activation upon glutamate stimulation prompts it to directly phosphorylate FOXO3a

Journal of Cell Science

Journal of Cell Science (2016) 129, 1815-1830 doi:10.1242/jcs.185009

at S43, S173, S294 and S325, which triggers its nuclear localization and subsequent activation. Cdk5 inhibition or depletion completely prevents Foxo3 localization and activation, thereby underscoring a major role of Cdk5 in this process. We further show that Cdk5-mediated phosphorylation of Foxo3 is required for its nuclear localization and activation. This finding is important as Cdk5 hyperactivation under neurotoxic conditions is known to cause nuclear dispersion, which mislocalizes several proteins including Cdk5 in the nucleus (Chang et al., 2011). However, phosphorylation-resistant 4A-FOXO3a remained in the cytoplasm in glutamate-treated cells (Fig. 4A), thereby confirming a mandatory role of phosphorylation in its nuclear migration.

The significance of Foxo3 activation was exemplified by its contribution towards two hallmarks of Alzheimer's disease, namely abnormal Aβ processing and neuronal death in glutamate-exposed HT22 cells and primary cortical neurons. We show that initially Foxo3 activation promotes the activation of MnSOD, but later promotes pro-apoptotic genes Bim and FasL leading to cell death. Furthermore, active Foxo3 also increases the activity of APP promoter and increases neurotoxic Aβ processing. Importantly, the phospho-resistant mutant of FOXO3a inhibits neurotoxic Aβ processing, suggesting that phosphorylation of Foxo3 is crucial for its neurotoxic role in Alzheimer's disease models. Our finding is consistent with a previous report showing that ectopic expression of nuclear-targeted Foxo3 causes neurotoxic Aβ formation in primary neurons (Qin et al., 2008). Finally, our *in vivo* data also supports increased levels and increased nuclear localization of Foxo3 in mouse brains upon Cdk5 activation, further underscoring the significance of this pathway in Alzheimer's disease pathogenesis. A recent study indeed showed increased levels of Foxo3 in the nuclei of neurons in mice with high fat diets where proapototic genes were activated (Nuzzo et al., 2015). Most importantly, these mice exhibited several Alzheimer's disease phenotypes including increased levels of APP, Aβ(1–40) and Aβ(1–42) along with BACE and tau proteins, which further exemplifies the significance of Foxo3 signaling in Alzheimer's disease pathogenesis.

A crucial role of deregulated Cdk5 in increasing neurotoxic Aβ processing has been observed previously. Deregulated Cdk5 phosphorylates APP at T668 which increases Aβ formation (Ando et al., 2001). Cdk5 deregulation mediated by p25 overexpression increases the transcription of BACE1 which causes amyloidogenic processing of APP leading to neurotoxic Aβ formation (Wen et al., 2008). Cdk5 also increases BACE1 activity by directly phosphorylating it at T252 (Song et al., 2015). Importantly, BACE1 and γ-secretase are highly enriched in lipid rafts (Riddell et al., 2001), and thus the subset of APP that resides in lipid rafts is subjected to amyloidogenic processing by BACE1. In contrast, the APP pool that resides in the non-raft region, is processed non-amyloidogenically by α-secretase. As our data show that Foxo3 increases APP promoter activity, it is likely that increased pool of APP in the lipid raft is cleaved by BACE1 leading to neurotoxic Aβ production. Future studies are needed to confirm this mechanism.

In conclusion, we show that deregulated Cdk5 is a major controller of Foxo3 signaling in HT22 cells, primary neurons and in an Alzheimer's disease mouse model. Activation of Foxo3 appears to be neuroprotective initially; however, later on it plays a crucial role in promoting cell death by upregulating Bim and FasL (Fig. 8D). Prevention of Foxo3 phosphorylation by Cdk5 confers significant neuroprotection, suggesting that inhibition of Cdk5 or activation of Akt to degrade FOXO3a might be an effective way to prevent or delay the irreversible process of neurodegeneration either alone or in combination.

MATERIALS AND METHODS

Glutamate, 3-(4,5-dimethyldiazol-2-yl)-2,5-diphenyltetrazolium bromide (MTT), and poly-l-lysine were obtained from Sigma. Roscovitine was purchased from LC Laboratories. Antibodies against Cdk5 (C-8), actin (C-2), Lamin A (H-102), Foxo3 (N-15), MAP2 (H300) and PSD95 (7E3) were purchased from Santa Cruz Biotechnology (Cai and Xia, 2008; Chang et al., 2011, 2012). All antibodies were used at 1:1000 dilution.

Cell culture

HT22 cells were a kind gift from David Schubert (Salk Institute, La Jolla, CA). HEK293T cells were purchased from the ATCC. HT22 cells, HEK293T and phoenix cells were cultured as reported previously (Sun et al., 2011). All cells were tested for potential contamination.

Isolation of primary cortical neurons

The primary cortical neurons were isolated from E17 CD1 mice embryos as reported previously (Chang et al., 2012). All the experiments were performed after 12 days in culture.

Expression plasmids and constructs

HA-tagged human FOXO3a was cloned into TAT-HA and VIP3 vectors at BamHI and Xho1 sites. HA-tagged FOXO3a mutants were generated using overlapping PCR.

Expression and purification of Cdk5, p25 and Foxo3

6×-His-Cdk5 and 6×-His-p25 was generated and purified as reported previously (Chang et al., 2012). 6×-His tagged wild-type and mutant FOXO3a were expressed in *E. coli* and purified according to our published procedures (Sun et al., 2008a,b).

Transfection and retroviral infection

For generating stable cell lines, HA-tagged wild-type and mutant FOXO3a plasmids were transiently transfected using calcium phosphate into Phoenix cells. The retroviruses were harvested and used to infect HT22 cells as reported previously (Shah and Shokat, 2002). For luciferase experiments, corresponding plasmids were transfected using Lipofectamine (Invitrogen) according to the manufacturer's instructions.

In vitro kinase assays

For *in vitro* labeling, 2 µg of 6×-His-tagged wild-type or mutant FOXO3a were incubated with Cdk5–p25 complex and 1 microCurie of [γ-^{32}P]ATP in a kinase buffer. Reactions were terminated by adding SDS sample buffer, separated by SDS-PAGE and transferred onto PVDF membranes and exposed for autoradiography.

Foxo3 shRNA

Cdk5 shRNA (mouse) was generated in our previous study (Chang et al., 2011). Foxo3 shRNA was cloned into pLKO.1 vector. Foxo3 shRNA (mouse) primer sequences were as follows: forward, 5′-CCGGGCTTCC-CATATACCGCCAAGACTCGAGTCTTGGCGGTATATGGGAAGCTT-TTTG-3′, and reverse, 5′-AATTCAAAAAGCTTCCCATATACCGCCA-AGACTCGAGTCTTGGCGGTATATGGGAAGC-3′. Control shRNA (scrambled shRNA), Cdk5 and Foxo3 shRNA lentiviruses were generated and used for infecting HT22 cells for 30 h.

Western blotting

Cells were lysed in modified RIPA buffer, supplemented with protease inhibitors. Equal amounts of cell extracts were used for western blotting.

MTT assay

Cells were seeded in 96-well plates at 5×10^3 cells per 100 µl per well and cultured for 24, 48 and 72 h. The MTT assay was conducted as reported previously (Sun et al., 2008a). Experiments were repeated three times in triplicate wells to ensure reproducibility.

Immunoprecipitation of Cdk5

HT22 cells were treated with 5 mM glutamate for 1.5 h, 3 h or 6 h. Cells were then harvested and lysed in RIPA buffer. After centrifugation (15,000 ***g***

for 20 min), whole-cell lysate was mixed with protein-A–Sepharose beads (Sigma) and anti-Cdk5 antibody. After incubation overnight, immunocomplexes were washed and then subjected to western blotting using either Cdk5 or Foxo3 antibodies.

Subcellular fractionation

Subcellular fractionation of HT22 cells was conducted as described previously (Chang et al., 2011).

Immunofluorescence

HT22 cells were grown on poly-L-lysine coated coverslips for 24 h followed by various treatments. Roscovitine (10 µM) was added 0.5 h before glutamate treatment and Cdk5 shRNA lentivirus was added 30 h prior to glutamate treatment. Cells were fixed with 4% formaldehyde in PBS for 15 min at room temperature, and then washed three times with PBS. The cells were blocked in 1% FBS, 2% BSA, 0.1% Triton X-100 in PBS for 1 h at 25°C. Cells were labeled with antibodies (against Cdk5 or Foxo3 or MAP2 or PSD95 or HA) for 3 h in PBS, followed by incubation with fluorescein-isothiocyanate- or Texas-Red-conjugated secondary antibody. Cells were visualized using a Nikon Eclipse E600 microscope (Nikon Instruments, Melville, NY).

Dual luciferase assay

HT22 cells or primary cortical neurons were plated in a 96-well plate. After 12 h, the cells were transfected with 47.5 ng/well of pGL3-based luciferase plasmids using Lipofectamine (Invitrogen). Cells were simultaneously transfected with 47.5 ng/well of the pRL-SV40 *Renilla* luciferase plasmid (Promega) as an internal control. For Cdk5 shRNA experiments, Cdk5 shRNA lentivirus was infected 24 h prior to luciferase plasmid transfection. At 48 h after transfection, 5 mM glutamate was added to the medium for varying periods (6 h, 12 h, 18 h, 24 h) in the presence or absence of roscovitine (10 µM) and firefly and *Renilla* luciferase activities were measured with the Dual-Luciferase kit (Thermo-scientific). The firefly luciferase signal was normalized to the *Renilla* luciferase signal to account for variations in transfection efficiency. All experiments were done in triplicate and repeated three independent times.

Measurement of β-amyloid release using ELISA

HT22 cells were transfected with APP-swe plasmid. Both APP-swe HT22 cells and primary cortial neurons were treated with glutamate for 18 h. The released β-amyloid was measured using SensoLyte® Anti-Humanβ-amyloid (1-42) Quantitative ELISA kit (Anaspec, CA) according to the manufacturer's instructions.

Immunocytochemistry in p25 transgenic mice

All the animal experiments in this study were reviewed and approved by the IACUC at Case Western Reserve University. We purchased CaMKII-tTA and tet-o-p25 mice (Cruz et al., 2003) from the Jackson Laboratory (Bar Harbor, ME), which were mated to generate p25-inducible transgenic mice. A doxycycline-containing diet (200 mg/kg; Bio-Serve, Frenchtown, NJ) was provided to prevent the induction of p25 until they reach 3–4 months of age. The expression of p25 was induced by replacing the doxycycline diet with a regular diet for 2 weeks. Immunocytochemistry in p25 transgenic mice was conducted according to our published procedure (Sun et al., 2009; Chang et al., 2010).

Statistical analysis

Bar graphs results are plotted as the mean±s.e.m. Significance was evaluated using Student's *t*-test analysis and is displayed as follows: $*P<0.01$.

Acknowledgements

We thank Dr David Schubert for HT22 cells and Dr Yanzhuang Wang for APP-swe plasmid. 1037pGL3 FasL promoter was a gift from William Sellers (Addgene plasmid # 9028) (Nakamura et al., 2000) and pLKO.1 TRC vector was a gift from David Root (Addgene plasmid # 10878) (Moffat et al., 2006). APP-luc plasmid was a gift from Dr Debomoy Lahiri. MnSOD-luc plasmid was a gift from Dr Daret St. Clair and Bim-luc plasmid was a gift from Dr Hisashi Harada.

Competing interests

The authors declare no competing or financial interests.

Author contributions

K.S. designed the study and wrote the paper. C.S. performed all tissue culture and primary neurons experiments. K.V. constructed wild-type and mutant FOXO3a plasmids, purified recombinant proteins, and conducted the kinase assays. H.G.L. conducted p25-transgenic animal studies. All authors analyzed the results and approved the final version of the manuscript.

Funding

This work was supported by a grant from National Institute on Aging, National Institutes of Health [grant number R21-AG 47447 to K.S. and H.-G.L.]. Deposited in PMC for release after 12 months.

References

Ando, K., Iijima, K.-I., Elliott, J. I., Kirino, Y. and Suzuki, T. (2001). Phosphorylation-dependent regulation of the interaction of amyloid precursor protein with Fe65 affects the production of beta-amyloid. *J. Biol. Chem.* **276**, 40353-40361.

Bibb, J. A., Chen, J., Taylor, J. R., Svenningsson, P., Nishi, A., Snyder, G. L., Yan, Z., Sagawa, Z. K., Ouimet, C. C., Nairn, A. C. et al. (2001). Effects of chronic exposure to cocaine are regulated by the neuronal protein Cdk5. *Nature* **410**, 376-380.

Cai, B. and Xia, Z. (2008). p38 MAP kinase mediates arsenite-induced apoptosis through Foxo3a activation and induction of Bim transcription. *Apoptosis* **13**, 803-810.

Calnan, D. R. and Brunet, A. (2008). The FoxO code. *Oncogene* **27**, 2276-2288.

Chang, K.-H., De Pablo, Y., Lee, H.-P., Lee, H.-G., Smith, M.-A. and Shah, K. (2010). Cdk5 is a major regulator of p38 cascade: relevance to neurotoxicity in Alzheimer's disease. *J. Neurochem.* **113**, 1221-1229.

Chang, K.-H., Multani, P. S., Sun, K.-H., Vincent, F., de Pablo, Y., Ghosh, S., Gupta, R., Lee, H.-P., Lee, H.-G., Smith, M. A. et al. (2011). Nuclear envelope dispersion triggered by deregulated Cdk5 precedes neuronal death. *Mol. Biol. Cell* **22**, 1452-1462.

Chang, K.-H., Vincent, F. and Shah, K. (2012). Deregulated Cdk5 triggers aberrant activation of cell cycle kinases and phosphatases inducing neuronal death. *J. Cell Sci.* **125**, 5124-5137.

Cruz, J. C., Tseng, H.-C., Goldman, J. A., Shih, H. and Tsai, L.-H. (2003). Aberrant Cdk5 activation by p25 triggers pathological events leading to neurodegeneration and neurofibrillary tangles. *Neuron* **40**, 471-483.

Dávila, D. and Torres-Aleman, I. (2008). Neuronal death by oxidative stress involves activation of FOXO3 through a two-arm pathway that activates stress kinases and attenuates insulin-like growth factor I signaling. *Mol. Biol. Cell* **19**, 2014-2025.

Dhavan, R. and Tsai, L.-H. (2001). A decade of CDK5. *Nat. Rev. Mol. Cell Biol.* **2**, 749-759.

Fischer, A., Sananbenesi, F., Pang, P. T., Lu, B. and Tsai, L.-H. (2005). Opposing roles of transient and prolonged expression of p25 in synaptic plasticity and hippocampus-dependent memory. *Neuron* **48**, 825-838.

Fukunaga, K., Ishigami, T. and Kawano, T. (2005). Transcriptional regulation of neuronal genes and its effect on neural functions: expression and function of forkhead transcription factors in neurons. *J. Pharmacol. Sci.* **98**, 205-211.

Gan, L., Zheng, W., Chabot, J.-G., Unterman, T. G. and Quirion, R. (2005). Nuclear/cytoplasmic shuttling of the transcription factor FoxO1 is regulated by neurotrophic factors. *J. Neurochem.* **93**, 1209-1219.

Haass, C., Lemere, C. A., Capell, A., Citron, M., Seubert, P., Schenk, D., Lannfelt, L. and Selkoe, D. J. (1995). The Swedish mutation causes early-onset Alzheimer's disease by beta-secretase cleavage within the secretory pathway. *Nat. Med.* **1**, 1291-1296.

Hawasli, A. H., Benavides, D. R., Nguyen, C., Kansy, J. W., Hayashi, K., Chambon, P., Greengard, P., Powell, C. M., Cooper, D. C. and Bibb, J. A. (2007). Cyclin-dependent kinase 5 governs learning and synaptic plasticity via control of NMDAR degradation. *Nat. Neurosci.* **10**, 880-886.

Hensley, K., Venkova, K., Christov, A., Gunning, W. and Park, J. (2011). Collapsin response mediator protein-2: an emerging pathologic feature and therapeutic target for neurodisease indications. *Mol. Neurobiol.* **43**, 180-191.

Hisanaga, S.-I. and Endo, R. (2010). Regulation and role of cyclin-dependent kinase activity in neuronal survival and death. *J. Neurochem.* **115**, 1309-1321.

Hoekman, M. F. M., Jacobs, F. M. J., Smidt, M. P. and Burbach, J. P. H. (2006). Spatial and temporal expression of FoxO transcription factors in the developing and adult murine brain. *Gene Expr. Patterns* **6**, 134-140.

Hosie, K. A., King, A. E., Blizzard, C. A., Vickers, J. C. and Dickson, T. C. (2012). Chronic excitotoxin-induced axon degeneration in a compartmented neuronal culture model. *ASN Neuro.* **4**, e00076.

Johnson, E. O., Chang, K. H., Ghosh, S., Venkatesh, C., Giger, K., Low, P. S. and Shah, K. (2012). LIMK2 is a crucial regulator and effector of Aurora-A-kinase-mediated malignancy. *J. Cell Sci.* **125**, 1204-1216.

Johnson, E. O., Chang, K. H., de Pablo, Y., Ghosh, S., Mehta, R., Badve, S. and Shah, K. (2011). PHLDA1 is a crucial negative regulator and effector of Aurora A kinase in breast cancer. *J. Cell Sci.* **124**, 2711-2722.

Kim, S. and Shah, K. (2007). Dissecting yeast Hog1 MAP kinase pathway using a chemical genetic approach. *FEBS Lett.* **581**, 1209-1216.

Kim, D., Frank, C. L., Dobbin, M. M., Tsunemoto, R. K., Tu, W., Peng, P. L., Guan, J. S., Lee, B. H., Moy, L. Y., Giusti, P., Broodie, N., Mazitschek, R., Delalle, I., Haggarty, S. J., Neve, R. L., Lu, Y. and Tsai, L. H. (2008). Deregulation of HDAC1 by p25/Cdk5 in neurotoxicity. *Neuron.* **60**, 803-817.

Klotz, L.-O., Sánchez-Ramos, C., Prieto-Arroyo, I., Urbánek, P., Steinbrenner, H. and Monsalve, M. (2015). Redox regulation of FoxO transcription factors. *Redox Biol.* **6**, 51-72.

Kops, G. J. P. L., Dansen, T. B., Polderman, P. E., Saarloos, I., Wirtz, K. W. A., Coffer, P. J., Huang, T.-T., Bos, J. L., Medema, R. H. and Burgering, B. M. T. (2002). Forkhead transcription factor Foxo3a protects quiescent cells from oxidative stress. *Nature* **419**, 316-321.

McLinden, K. A., Trunova, S. and Giniger, E. (2012). At the fulcrum in health and disease: Cdk5 and the balancing acts of neuronal structure and physiology. *Brain Disord. Ther.* **Suppl. 1**, 001.

Meijer, L., Borgne, A., Mulner, O., Chong, J. P. J., Blow, J. J., Inagaki, N., Inagaki, M., Delcros, J.-G. and Moulinoux, J.-P. (1997). Biochemical and cellular effects of roscovitine, a potent and selective inhibitor of the cyclin-dependent kinases cdc2, cdk2 and cdk5. *Eur. J. Biochem.* **243**, 527-536.

Meyer, D. A., Torres-Altoro, M. I., Tan, Z., Tozzi, A., Di Filippo, M., DiNapoli, V., Plattner, F., Kansy, J. W., Benkovic, S. A., Huber, J. D. et al. (2014). Ischemic stroke injury is mediated by aberrant Cdk5. *J. Neurosci.* **34**, 8259-8267.

Moffat, J., Grueneberg, D. A., Yang, X., Kim, S. Y., Kloepfer, A. M., Hinkle, G., Piqani, B., Eisenhaure, T. M., Luo, B., Grenier, J. K., et al. (2006). A lentiviral RNAi library for human and mouse genes applied to an arrayed viral high-content screen. *Cell* **124**, 1283-1298.

Morel, M., Authelet, M., Dedecker, R. and Brion, J. P. (2010). Glycogen synthase kinase-3beta and the p25 activator of cyclin dependent kinase 5 increase pausing of mitochondria in neurons. *Neuroscience* **167**, 1044-1056.

Nakamura, N., Ramaswamy, S., Vazquez, F., Signoretti, S., Loda, M. and Sellers, W. R. (2000). Forkhead transcription factors are critical effectors of cell death and cell cycle arrest downstream of PTEN. *Mol. Cell. Biol.* **20**, 8969-8982.

Nikolic, M., Dudek, H., Kwon, Y. T., Ramos, Y. F. and Tsai, L. H. (1996). The cdk5/p35 kinase is essential for neurite outgrowth during neuronal differentiation. *Genes Dev.* **10**, 816-825.

Nuzzo, D., Picone, P., Baldassano, S., Caruana, L., Messina, E., Marino Gammazza, A., Cappello, F., Mulè, F. and Di Carlo, M. (2015). Insulin resistance as common molecular denominator linking obesity to Alzheimer's disease. *Curr. Alzheimer Res.* **12**, 723-735.

Peng, S., Zhao, S., Yan, F., Cheng, J., Huang, L., Chen, H., Liu, Q., Ji, X. and Yuan, Z. (2015). HDAC2 selectively regulates foxo3a-mediated gene transcription during oxidative stress-induced neuronal cell death. *J. Neurosci.* **35**, 1250-1259.

Qin, W., Zhao, W., Ho, L., Wang, J., Walsh, K., Gandy, S. and Pasinetti, G. M. (2008). Regulation of forkhead transcription factor FoxO3a contributes to calorie restriction-induced prevention of Alzheimer's disease-type amyloid neuropathology and spatial memory deterioration. *Ann. N. Y. Acad. Sci.* **1147**, 335-347.

Riddell, D. R., Christie, G., Hussain, I. and Dingwall, C. (2001). Compartmentalization of beta-secretase (Asp2) into low-buoyant density, noncaveolar lipid rafts. *Curr. Biol.* **11**, 1288-1293.

Sanphui, P. and Biswas, S. C. (2013). FoxO3a is activated and executes neuron death via Bim in response to β-amyloid. *Cell Death Dis.* **4**, e625.

Shah, K. and Lahiri, D. K. (2014). Cdk5 activity in the brain - multiple paths of regulation. *J. Cell Sci.* **127**, 2391-2400.

Shah, K. and Shokat, K. M. (2002). A chemical genetic screen for direct v-Src substrates reveals ordered assembly of a retrograde signaling pathway. *Chem. Biol.* **9**, 35-47.

Shah, K. and Vincent, F. (2005). Divergent roles of c-Src in controlling platelet-derived growth factor-dependent signaling in fibroblasts. *Mol. Biol. Cell* **16**, 5418-5432.

Shukla, V., Skuntz, S. and Pant, H. C. (2012). Deregulated Cdk5 activity is involved in inducing Alzheimer's disease. *Arch. Med. Res.* **43**, 655-662.

Song, W.-J., Son, M.-Y., Lee, H.-W., Seo, H., Kim, J. H. and Chung, S.-H. (2015). Enhancement of BACE1 activity by p25/Cdk5-mediated phosphorylation in Alzheimer's disease. *PLoS ONE* **10**, e0136950.

Sun, K.-H., de Pablo, Y., Vincent, F., Johnson, E. O., Chavers, A. K. and Shah, K. (2008a). Novel genetic tools reveal Cdk5's major role in Golgi fragmentation in Alzheimer's disease. *Mol. Biol. Cell* **19**, 3052-3069.

Sun, K.-H., de Pablo, Y., Vincent, F. and Shah, K. (2008b). Deregulated Cdk5 promotes oxidative stress and mitochondrial dysfunction. *J. Neurochem.* **107**, 265-278.

Sun, K.-H., Lee, H.-G., Smith, M. A. and Shah, K. (2009). Direct and indirect roles of Cyclin-dependent Kinase 5 as an upstream regulator in the c-Jun NH2-terminal kinase cascade: relevance to neurotoxic insults in Alzheimer's disease. *Mol. Biol. Cell* **20**, 4611-4619.

Sun, K.-H., Chang, K.-H., Clawson, S., Ghosh, S., Mirzaei, H., Regnier, F. and Shah, K. (2011). Glutathione S-transferase P1 is a critical regulator of Cdk5 kinase activity. *J. Neurochem.* **118**, 902-914.

Sun, X., Jin, L. and Ling, P. (2012). Review of drugs for Alzheimer's disease. *Drug Discov. Ther.* **6**, 285-290.

Uranga, R. M., Katz, S. and Salvador, G. A. (2013). Enhanced phosphatidylinositol 3-kinase (PI3K)/Akt signaling has pleiotropic targets in hippocampal neurons exposed to iron-induced oxidative stress. *J. Biol. Chem.* **288**, 19773-19784.

Wang, S., Chong, Z. Z., Shang, Y. C. and Maiese, K. (2013). WISP1 neuroprotection requires FoxO3a post-translational modulation with autoregulatory control of SIRT1. *Curr. Neurovasc. Res.* **10**, 54-69.

Wang, X., Wang, Z., Chen, Y., Huang, X., Hu, Y., Zhang, R., Ho, M. S. and Xue, L. (2014). FoxO mediates APP-induced AICD-dependent cell death. *Cell Death Dis.* **5**, e1233.

Wen, Y., Yu, W. H, Maloney, B., Bailey, J., Ma, J., Marié, I., Maurin, T., Wang, L., Figueroa, H., Herman, M. et al. (2008). Transcriptional regulation of beta-secretase by p25/cdk5 leads to enhanced amyloidogenic processing. *Neuron* **57**, 680-690.

Whiteman, I. T., Gervasio, O. L., Cullen, K. M., Guillemin, G. J., Jeong, E. V., Witting, P. K., Antao, S. T., Minamide, L. S., Bamburg, J. R. and Goldsbury, C. (2009). Activated actin-depolymerizing factor/cofilin sequesters phosphorylated microtubule-associated protein during the assembly of alzheimer-like neuritic cytoskeletal striations. *J. Neurosci.* **29**, 12994-13005.

Zhu, W., Bijur, G. N., Styles, N. A. and Li, X. (2004). Regulation of Foxo3a by brain-derived neurotrophic factor in differentiated human SH-SY5Y neuroblastoma cells. *Brain Res. Mol. Brain Res.* **126**, 45-56.